FINAL: Decadal oscillation in the predictability of Palmer Drought Severity Index in California

Lelys Bravo[1], Mariangel garcia[2], gianni.bellocchi[3], and scodalabdiodato[3]

[1]Northern Illinois University
[2]San Diego State University
[3]Affiliation not available

October 7, 2018

Abstract

Drought in California is very variable from year-to-year and is highly influenced by precipitation in winter months, causing up to billions of dollars of damage in a single drought year. Improved understanding of the variability of drought on decadal and longer timescales is then essential to regional water resources planning and management in this U.S. state. This is a predictability study of the Palmer Drought Severity Index (PDSI) based on a time-series of annual data, started in 1801 to 2014, and projected for the time-horizon 2015-2054. An ensemble smoothing forecast was developed with an exponential smoothing model with seasonal component. The model was implemented for forecasting 40 years of the PDSI index. Results were compared with a linear transfer function model approach in where the Pacific Decadal Oscillation (PDO) index and Nino3.4 index are both used as input time series in the transfer function model. Both approaches result in a Mean Absolute Standardized Error (MASE) lower than 1 and similar Root Mean Square error (RMSE).

1. Introduction

Drought is a fundamental feature of the climate of western North America, where several regions of western United States (U.S.) have experienced protracted decadal-scale dry periods in the past centuries (Griffin and Anchukaitis, 2014b). Hydrologic droughts in western U.S. were already widespread and persistent during the so-callled Medieval Climate Anomaly, roughly in the period 900–1300 AD (**Meko et al., 2007**), with megadrought in southern California during 832-1074 AD and 1122-1299 AD (**Raab and Larson, 1997; Heusser et al., 2015**). Multi-year droughts have also recurred in more recent times, e.g. in 1818-1824, 1827-1829, 1841-1848 and 1855-1865, causing tremendous disruption on social, agricultural, ecological and economic fronts (**Cole et al., 2002**, Fig. 1).

In particular, the extreme drought which occurred in 1827-1829 caused death in livestock with thousands of animals died in plains (**Guin, 1890**). It followed five major droughts, which ended in 1924, 1935, 1950, 1960 and 1977. As well, the one started in 2012 (Griffin and Anchukaitis, 2014a) has generated a large pulse of tree mortality (**USFS, 2015**). How drought may change in future is of great concern as global warming continues (**Dai and Zhao, 2016**). Yet, how has an extreme drought occurrence over California shifted as a result of the change in climate since historical times? How can we see droughts coming? If we are dry during one drought year, will we likely be dry for other drought years, and then for a decade or more? How cyclical will these patterns be and how are they predictable over multidecadal time-scales? To answer these questions, we examined (with focus on California) the uncertainties in estimating future ramifications of drought years, and how drought changes can replicate over a near-future time-horizon using the Palmer Drought Severity Index (PDSI).
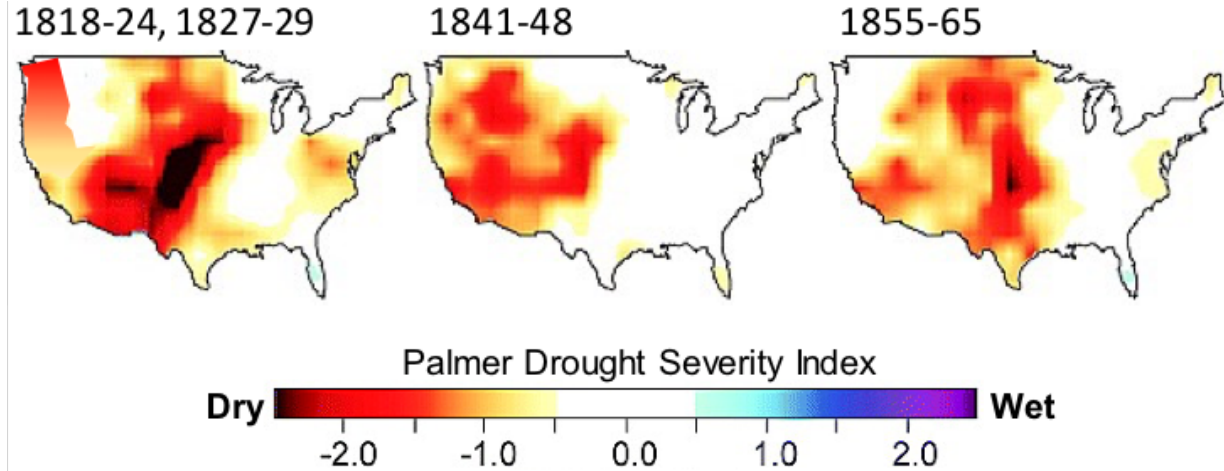
Figure 1: Mapped patterns of reconstructed PDSI for some intervals in 19th century across the U.S. (modified from Cole et al., 2002).

Many drought indices have been developed for the purpose of drought monitoring, based on meteorological and hydrological variables which show the size, duration, severity and spatial extent of droughts. The PDSI is such an example. It was developed by Palmer (1965) and it is one of the most well-known and widely used drought indices in the U.S. (e.g. Karl and Koscielny 1982, Byun and Wilhite 1999) and beyond (Dai et al. 1998, 2004; Shabbar and Skinner 2004; Tatli 2015; **Skinner, 2004; van der Schrier et al., 2006**). PDSI values are computed along the soil moisture balance that requires time series of temperature, precipitation, ground moisture content (or available water-holding capacity) and potential evapotranspiration. The calculation algorithm of PDSI - either in its original version by Palmer (1965) or in modified ones (e.g. Wells et al. 2004) - is thus a reflection of how much soil moisture is currently available compared to that for normal or average conditions. The PDSI incorporates both precipitation and temperature data in a simplified, though reasonably realistic, water balance model that accounts for both supply (rain or snowfall water equivalent) and demand (temperature, transformed into units of water lost through evapotranspiration), which affect the content of a two-layer soil moisture reservoir model (a runoff term is also activated when the reservoir is full). Not explicitly bounded, the PDSI typically falls in the range from -4 (extreme drought) to +4 (extremely wet). This dimensionless quantity allows the PDSI to be compared between regions with radically different precipitation regimes.

Land-atmosphere interactions can introduce persistence into droughts because reduced precipitation lowers soil moisture, reduces surface evapotranspiration and, with less vapor in the atmosphere, further reduces precipitation. In this sequence, soil moisture adjustment occurs with a length of time which introduces a lag and a memory. Depending on situations, there might be a strong coupling between soil moisture and precipitation, and land surface processes can lead to persistence (Koster et al., 2004). The calculation of PDSI is intended to model persistence in the soil moisture balance. The combination of past wet/dry conditions with past PDSI data means that the PDSI for a given time step (generally one month) can be seen as a weighted function of current moisture conditions and a contribution of PDSI over previous times (Cook et al., 2007). In the light of this persistence structure, PDSI chronologies can be used to reconstruct drought conditions, but persistence can also be a criterion to be used as a measure of predictability (Tatli, 2015).

This paper deals with time series analysis (TSA) related to PDSI dynamics. Several statistical TSA approaches have been applied to predict climate variables, including their extremes (**e.g. Han et al., 2012; Huang et al., 2014**). The potential ability of these modeling approaches to forecast drought has been

demonstrated by **Mossad and Alazba (2015)**. However, drought forecasts are often performed at monthly time-scale **(e.g., Mishra and Desai, 2005; Fernández et al., 2009)**. Here, we target annual to decadal time scales. We investigate to what extent TSA model simulations may give accurate forecasts of future hydrological changes. Although research on meteorological drought is particularly difficult because of the complex and heterogeneous character of drought processes, their temporal trends respond to climate fluctuations (e.g. large-scale atmospheric circulations). Specifically, the work explores a homogenized long series of annual PDSI data (1801-2014) as derived for California by Griffin and Anchukaitis (2014a). Then the study assesses the response of an Exponential Smoothing (ES) model, using an Ensemble Prediction approach. ES (Holt, 2004)**(Gardner, 2006)** and autoregressive integrated moving average (ARIMA) models **(Box and Jenkins, 1970)** are the most representative methods in TSA. In this study, ES was used because it is known to be optimal for a broader class of state-space models than ARIMA models **(Gardner, 2006)**. ES responds easily to changes in the pattern of time series (McClain, 1974) and is often referred to as a reference model for time-pattern propagation into the future (Taylor, 2003; Hyndman et al., 2008). It is also less complex in its formulation and, as such, it was expected to be easier in identifying the causes of unexpected results. The ensemble approach has been adopted as a way to consider uncertainty in hydrological forecasting, and thus enhance accuracy by combining forecasts made at different lead times, as in Armstrong (2001b) and in previous authors' papers (e.g. Diodato 2014; Diodato et al. 2017 and Diodato and Bellocchi 2014). A lengthy PDSI series offers a unique opportunity to explore past interannual-to-interdecadal climate variability, and to use its internal dependence structure to (try to) replicate future PDSI ramifications. This approach is compared with the more traditional TSA approach using transfer function models, introduced by **Box and Jenkins (1970)** and re-visited by Shumway and Stoffer (2017a). In this case input time series of El Niño Southern Oscillation (ENSO) and the the Pacific Decadal Oscillation (PDO) are considered as impulse inputs to the output PDSI time series. An approximate ensemble approach is also developed under the transfer function models framework for comparison purposes with the ES results.

The paper is organized along the following lines. Data resources and modeling approaches are described in Section . The empirical results on data analysis and ensemble forecasts are described in Section . A comparison of the ES model with the transfer function modeling approach is presented in Section . The results are discussed and put in perspective with previous studies in Section , which closes the paper with some concluding remarks.

2. Material and methods

2.1 Environmental setting and data

The California's climate varies widely, from hot desert to subarctic, depending on latitude, elevation, and proximity to the coast. California's coastal regions, the Sierra Nevada foothills, and much of the Central Valley have a Mediterranean climate, with warm to hot, dry summers and mild, moderately wet winters (Fig. 2a, b). The influence of the ocean generally moderates temperature extremes, creating warmer winters and substantially cooler summers in coastal areas. The rainy period in most of the country as well as in Teheran is from November to May (Fig. 2a).

Prevailing westerly winds from the Pacific Ocean also bring moisture. The average annual rainfall in California is about 350 mm, with the northern parts of the state generally receiving higher rain amounts than the south. The reference evapotranspiration follows a more complex pattern, mostly in relation to elevation and distance from sea (Fig. 2c). Temperature and evapotranspiration are especially important in California, where water storage and distribution systems are critically dependent on winter/spring rainfall, and excess demand is typically met by groundwater withdrawal **(Diffenbaugh et al., 2015)**. The PDSI time series derived from Griffin and Anchukaitis (2014a) reconstructed drought for California.
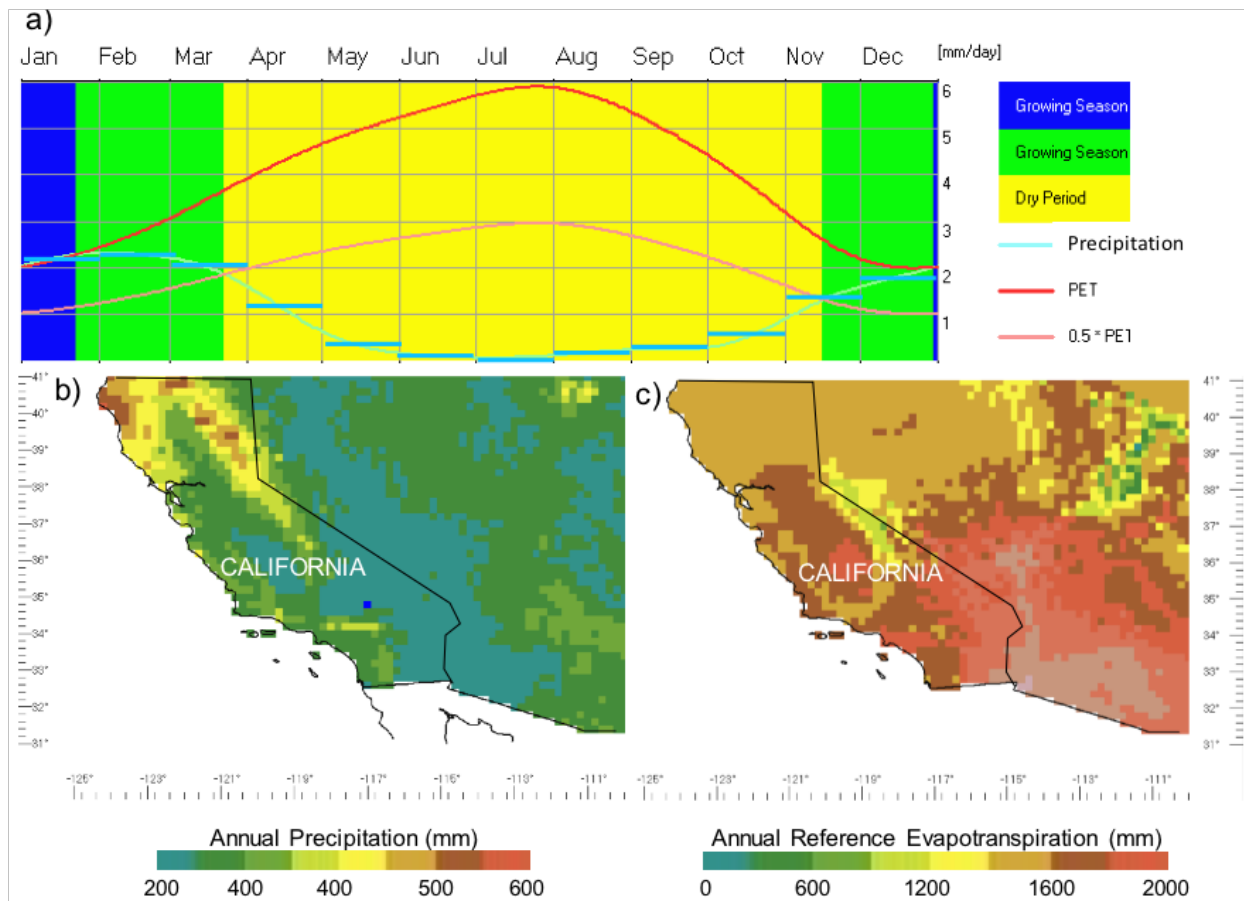
Figure 2: Rainfall monthly regime with relative bioclimatic patterns for California a); mean annual smoothed 20-km spatial precipitation over the period 1961-1990 b) and the corresponding annual reference evapotranspiration c) (arranged via LocClim FAO software).

2.2 Statistical model

Exponential Smoothing

Among the forecast equations for all time series-based estimates, the exponential smoothing (a popular scheme to produce smoothed time series) is a relatively simple prototype model for forecasting, analysis and re-analysis of environmental variables (**Box, 1991**; Montgomery et al., 2008). This technique uses historical time series data under the assumption that the future will like resemble the past, in an attempt to identify specific patterns in the data and then project and extrapolate those patterns into the future (without using the model to identify the causes of patterns). Compared to other techniques (e.g. moving averages), which equally weight past observations, exponential smoothing apportions exponentially decreasing weights as observations get older. This means that recent observations are given relatively more weight in forecasting than older observations. To compute predictions based on the observed time series of PDSI data, we make use of our knowledge concerning the period of the system under investigation (e.g. Wichard and Merkwirth, 2005). The following periodic simple exponential smoothing Taylor (2003) was selected as reference model for time-pattern propagation into the future:

$$F(X)_{t+m}^R = \alpha \frac{X_t}{I_{t-p}}$$

where $F(y)$ represents the m-step-ahead forecast from PDSI $\{X_t\}$ on N years for ensemble (Rth)–runs; S_t is the smoothed PDSI at decadal scale centred on time-year t. is the actual PDSI; α is the smoothing parameter for the data; I_{t-p} is the smoothed cycle index at the end of period t with its number defined by the the number of periods (p) in the seasonal cycle:

$$F(I)_{t-p}^R = \delta \frac{X_t}{S(X)_{t-p}} + (1-\delta)I_{t-1}$$

where δ is smoothing parameter for cyclical indices.

Transfer Function Models

An alternative methodology based on transfer function (TF) models was also implemented to compare two methodologies: seasonal exponential smoothing that uses the temporal dependence structure of the time series itself to reproduce the time series behavior in the future, versus the linear transfer function approach where input time series potentially impacting the drought behavior at large spatial scales are used as explanatory time serie variables in a lagged regression model. The methodology called transfer fuction models, was introduced by Box and Jenkins (1976) and re-visited by Shumway and Stoffer, 2017a to model the impact of El Niño on fish recruitment and for de Guenni et al. (2016) to forecast monthly rainfall in the coast of Ecuador based on El Niño indexes.

In a transfer function model the output series $Y(t)$ (in this case PDSI) can be represented as:

$$Y(t) = \alpha_1(B)X_1(t) + \alpha_2(B)X_2(t) + ... + \alpha_k(B)X_k(t) + \eta(t)$$

where $X_1(t), X_2(t), ..., X_k(t)$ are the input time series to be considered as explanatory variables contributing to the temporal dynamics of the output series $Y(t)$ and $\eta(t)$ is a stationary random process. The terms $\alpha_1(B), \alpha_2(B), ..., \alpha_k(B)$ are fractional polynomials in the back-shift operator B (such that $B^s(X(t)) = X(t-s)$) of the form:

$$\alpha_i(B) = \delta_i(B)B^{d_i}/\omega_i(B)$$

where $\delta_i(B) = (\delta_{0i} + \delta_{1i}B^1 + ... + \delta_{si}B^{s_i})$ and $\omega_i(B) = (1 - \omega_{1i}B^1 - ... - \omega_{ri}B^{r_i})$ and s_i, r_i and d_i are the orders of the transfer function for each input time series $X_i(t)$. The numerator polynomial (order s_i) controls the lagged effect of the input variable $X_i(t)$ on the output time series; and the denominator (order r_i) controls the lagged effect of variable $Y(t)$ induced by $X_i(t)$. The backshift operator order d_i and the orders s_i and r_i are estimated by calculating the cross-correlation function between the pre-whitened input time series $X_i(t)$ (using an ARIMA model, such that the filter $\Phi(B)/\Theta(B)$ applied to $X_i(t)$ produces a white noise $v(t)$) and the filtered output series $\tilde{Y}(t)$ by applying the same ARIMA filter to the input time series. Once the orders s_i, r_i and d_i are identified, the corresponding linear transfer function is fitted using the R software. In our case $i = 1, 2$, since two input time series are used as covariates.

Model Validation Methods

To ensure the optimal runs over the hold back prediction (testing validation), model parameterization was achieved by minimizing together the Root Mean Squared Error (RMSE) and the Mean Absolute Scaled Error (MASE), and maximizing the correlation coefficient (R):

$$\begin{cases} min| & \text{RMSE} \\ min| & \text{MASE} \\ max| & \text{R} \end{cases}$$

The commonly used RMSE (Fox, 1981) quantifies the differences between predicted and observed values, and thus indicates how far the forecasts are from actual data. A few major outliers in the series can skew the RMSE statistic substantially because the effect of each deviation on the RMSE is proportional to the size of the squared error. The overall, nondimensional measure of the accuracy of forecasts MASE (Hyndman and Koehler, 2006) is less sensitive to outliers than the RMSE. The MASE is recommended for determining comparative accuracy of forecasts (Franses, 2016) because it examines the performance of forecasts relative to a benchmark forecast. It is calculated as the average of the absolute value of the difference between the forecast and the actual value divided by the scale determined by using a random walk model (naïve reference model on the history prior to the period of data held back for model training). MASE<1 indicates that the forecast model is superior to a random walk.

The correlation coefficient between estimates and observations Addiscott and Whitmore (1987), (-1 anti-correlation) $-1 \leq R \leq 1$ (1 perfect correlation), assesses linear relationships, in that forecasted values may show a continuous increase or decrease as actual values increase or decrease. Its extent is not consistently related to the accuracy of the estimates. Forecasts online means were used to employ simulation model with support of Excel spreadhseet. The statistics were assessed interactively using Statistics Software STATGRA-PHIC Online and WESSA R–JAVA web (Wessa, 2012).

In order to quantify long-range dependence and appraise the cyclical-trend patterns in the series, we estimated the Hurst H exponent (rate of chaos)(**add reference**) , which is related to the fractal dimension ($D = 2-H$) of the series. Long memory occurs when $0.5 < H < 1.0$, that is, events that are far apart are correlated because correlations tend to decay very slowly. On the contrary, short-range dependence $0.5 < H < 1.0$ is characterized by quickly decaying correlations, i.e. past trends tend to revert in the future (an up value is more likely followed by a down value). Calculating the Hurst exponent is not straightforward because it can only be estimated and several methods are available to estimate it, which often produce conflicting estimates (Karagiannis et al., 2002). Using SELFIS, we have referred to two methods, which are both credited to be good enough to estimate H Belov (2006) the widely used (Yin et al., 2009) rescaled range analysis (R/S method) and the ratio variance of residuals method, which is known to be unbiased almost through all Hurst range (Sheng and Chen, 2009). Long-memory in the occurrence of PDSI values was also analyzed to see if the memory characteristic is correlated with the length of the time series. To determine whether this characteristic changes over time, the Hurst exponent was not only estimated for the full time series (1801-2014), but also for a shorter series starting in 1901 (the most recent period, which is also the period held out of the calibration process).

3. Results

3.1 Data analysis

The first step in any time-series analysis and forecasting is to plot the observations against time, to gain an insight into possible trends and/or cycles associated with the temporal evolution of datasets. For our PDSI time series, Fig. 3a shows that the series presents important inter-annual and decadal variability, with smooth changes in its structure and turning points which help in orienting the choice of the most appropriate forecasting method (after Chatfield, 2000).
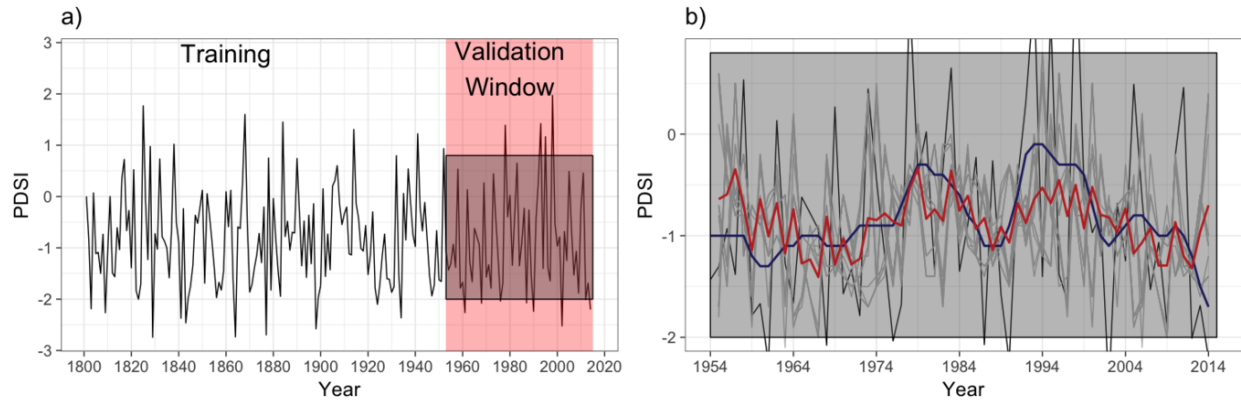

Figure 3: Observed Palmer Drought Severity Index time-series (blue curve 1801-2014) with training and validation periods (a), and, for the validation period, the simulated series (plume) with both the ensemble mean (red curve) and the observed Gaussian Filter with 11-year smoothing (bold black curve) b).

The smoothed series periodogram is presented in Fig 4 showing that most of the total variability in the series is associated to both short and large frequencies.

4

The whole of the PDSI time series (214 years of data from 1801 to 2014) was segregated into sub-sets for the purposes of training and validation (Fig. 3a). Forecasts were performed for the 40-year follow-up period (Fig. 3b). Alternative initial conditions were simulated for each run, taking periods with a different start year (in 10-year steps-up from year 1801 to 1900) and periodical cycles (41, 42 and 43 years) for model training (training datasets).

For 1954-2014 (Fig. 3b), the simulation results for validation testing are quite promising, judging by the closeness of ensemble prediction mean (red curve) to the observed 11-year Gaussian Filter (black curve) PDSI evolution.

The results indicate that the exponential model performs well at both high and low frequency variability, which is consistent with inter-annual to inter-decadal climate-variability. In fact, the residuals between predicted and observed time-series are coherent in the validation period: residual histograms and Q-Q plots do not identify substantive departures from normality in both official run (Fig. 5a, a_1) and ensemble mean (Fig. 5b, b_1).

The data are somewhat right-skewed; however, the right tail of the distribution is fairly closely approximated by the normal distribution, with some high extreme values.
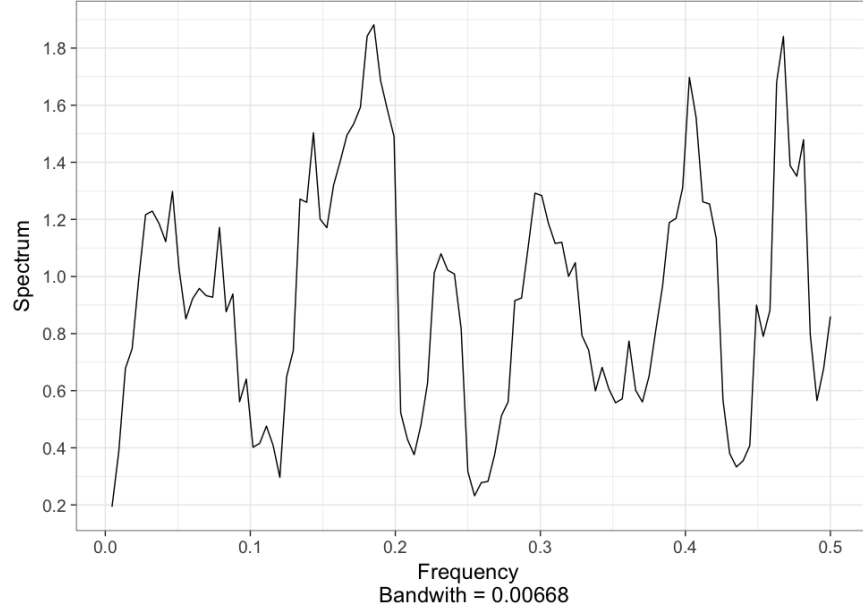
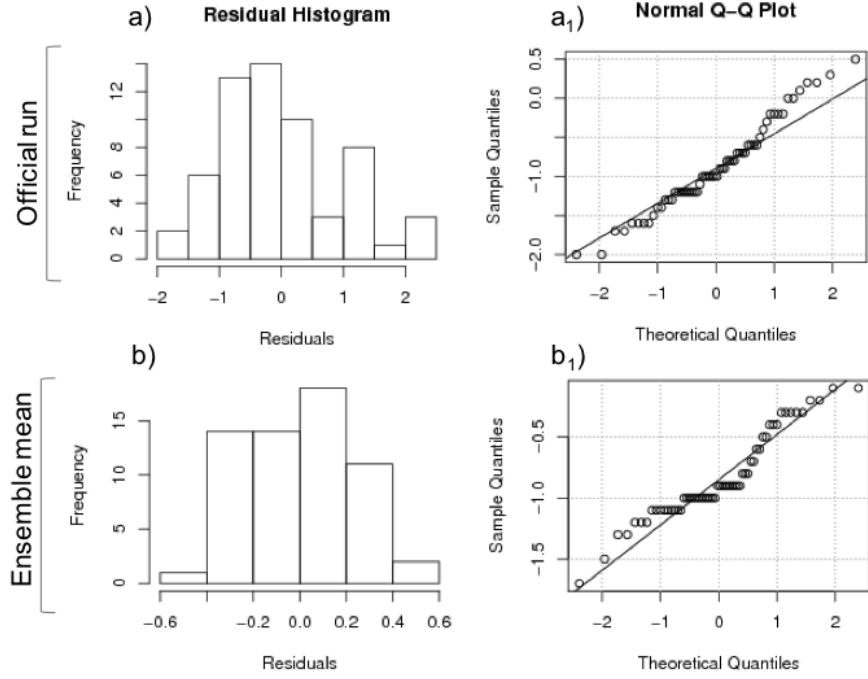Figure 4: Smoothed periodogram of the PDSI time series

Figure 5: Residual histogram and normal QQ Plot between PDSI forecasted and observed in validation period for official run (a, a_1) and ensemble mean (b, b_1).

In the validation stage, RMSE and MASE were equal to 1.0 and 0.68, respectively, which indicate a satisfactory performance and that the forecast model is superior to a random walk ($MASE < 1$)

With the R/S method, the Hurst exponent (H) was found to be greater than 0.6 in both the whole series (0.611) and the sub-set 1901-2014 (0.743), which is around the threshold of 0.65 used by Quian and Rasheed (2004) to identify series than can be predicted accurately. In the case of variance of residuals, we have a situation in which obtained results are hard for interpretation. For the whole of the series, the result ($H < 0.380$) is contradictory to our finding that the Hurst exponent is > 0.5 with R/S method and variance of residuals method in the sub-set 1901-2014 (0.611 and 0.550, respectively). With an increase of the number of series terms (amount of observations), the Hurst exponent is expected to get closer to 0 (Kaklauskas and Sakalauskas, 2013), i.e. the memory effect decreases. However, with the variance residuals method, the estimated Hurst exponent moves away from 0.5 ($H = 0.38$) with the whole of the time series. These contradictory results can be reconciled by considering that a complex concept such PDSI is hardly captured by one metric, the Hurst exponent, which (depending on the estimation method used) may not reflect the changes of heading direction (Dotov et al., 2016). Indeed, the whole of the series (Fig. 2a) shows frequent and sudden pulses of drought, with a change-point in 1917, as identified by the Buishand test (Buishand, 1982), observed in coincidence with the early 20th century pluvial centered on 1915(Cook et al., 2007), which has received much attention in the western U.S. (Woodhouse et al., 2005). By combining these results, it can be stated that the California's PDSI series is related with either a short-range ($H < 0.5$) or a long-range ($H > 0.5$) memory (in turn reflecting influences on the occurrence of droughts of both large-scale and small-scale climate systems), which assumes that some dependence structure exists that advocates the foreseeability of the series. We thus performed our forecasting analysis on the original time series of PDSI data.

3.2 Simulation experiment

Once the performance of the exponential smoothing model was established, the model trained over 1801-2014 periods was run to produce an ensemble of forecast paths of annual PDSI for 2015-2054. Our major interest was directed towards assessing the predictability of interdecadal variations.

Several forecast members show for the coming decades (Fig. ??) some trajectories following a ciclycal pattern, in which PDSI may fall below and above "incipient drought", with negligible monotonic, long-term trend. However, moving forward, ongoing changes in atmospheric circulation and associated precipitation and temperature variability in the western U.S. raise questions about the stationarity of extreme drought estimates (Robeson, 2015).

When examining the projection of PDSI over the four future decades (2015-2054), the ensemble mean value (Fig. ??, black bold curve) is observed to roughly lie around the "incipient drought" class, approaching "mild drought" around 2030, although some members push to "extreme drought". Around 2020 and 2036, PDSI forecasts approach "near normal" with some members which are inclined up to "incipient wet spell". After the year 2040, the PDSI resumes to decrease and remains below the "incipient drought" for years.

4. Comparison with the Transfer Function Modeling approach

El Niño Southern Oscillation (ENSO) has an important influence on the rainfall regime in California and most of the US with most dramatic impacts during the winter (Ropelewski and Halpert, 1986). The Pacific Decadal Oscillation (PDO) encompasses the ocean temperatures in the northern part of the ocean including variability modes at different temporal scales. The PDO has a warm phase and a cool phase. Each phase can last anywhere from a few years to decades. The cool phase is linked to dry conditions in Southern California and neighboring states (Patzert, 2015). Forget El Niño, the 'PDO' could be the real drought buster...
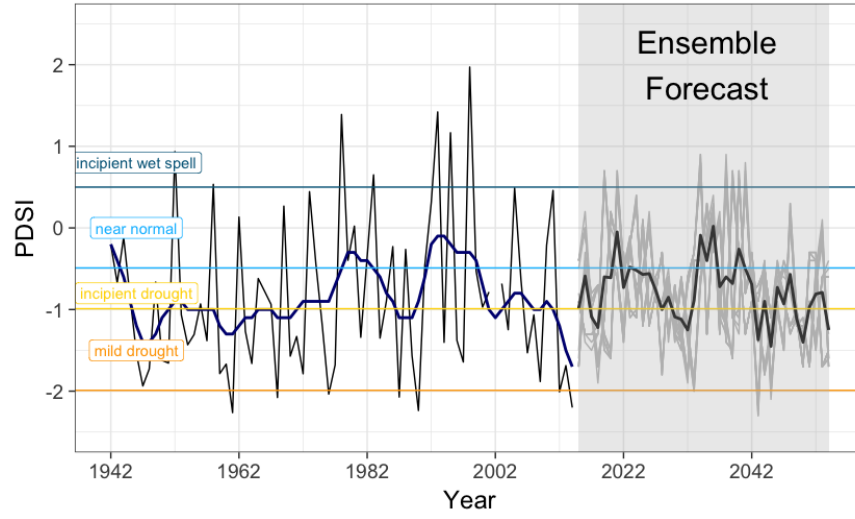
Figure 6: Evolution of observed annual PDSI (blue curve) with its smoothed 11-year Gaussian filter in bold black curve (1942-2014), and exponential smoothing forecasts with plume prediction. PDSI classes are also reported.

ENSO times series and PDO time series were available from the NOAA website. A plot of all ENSO time series jointly with the PDSI time series is shown in Figure 7.
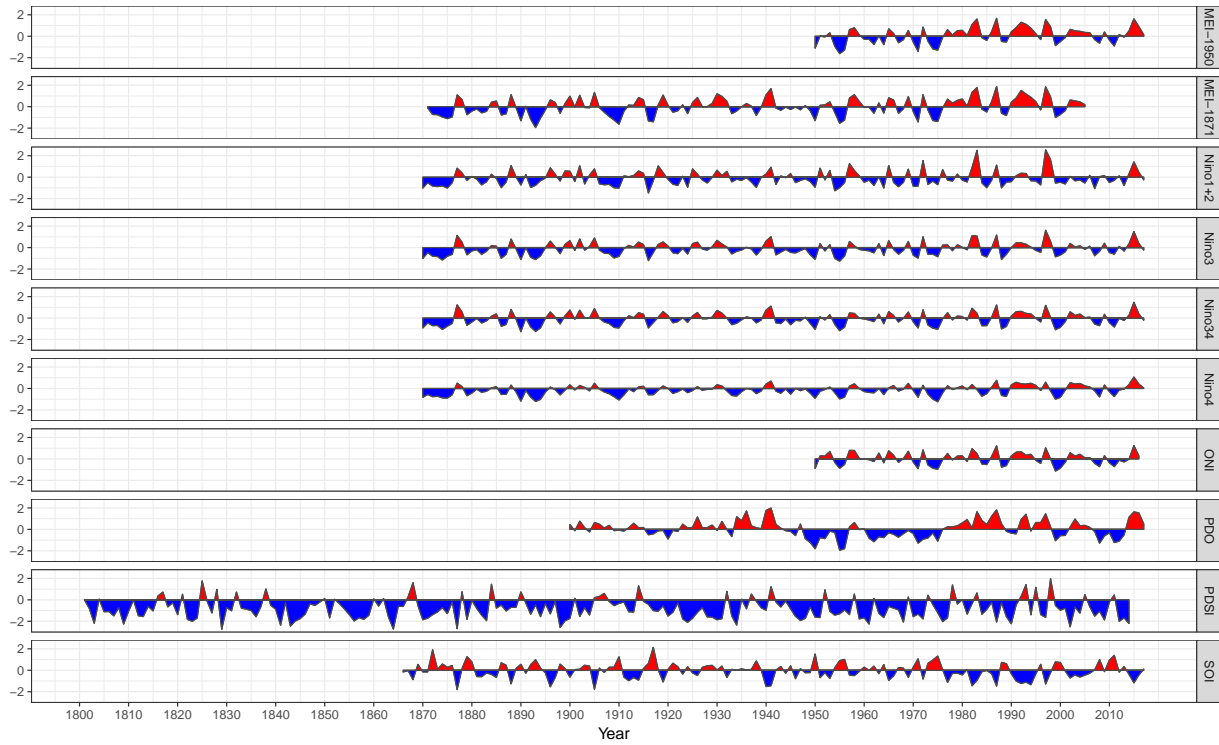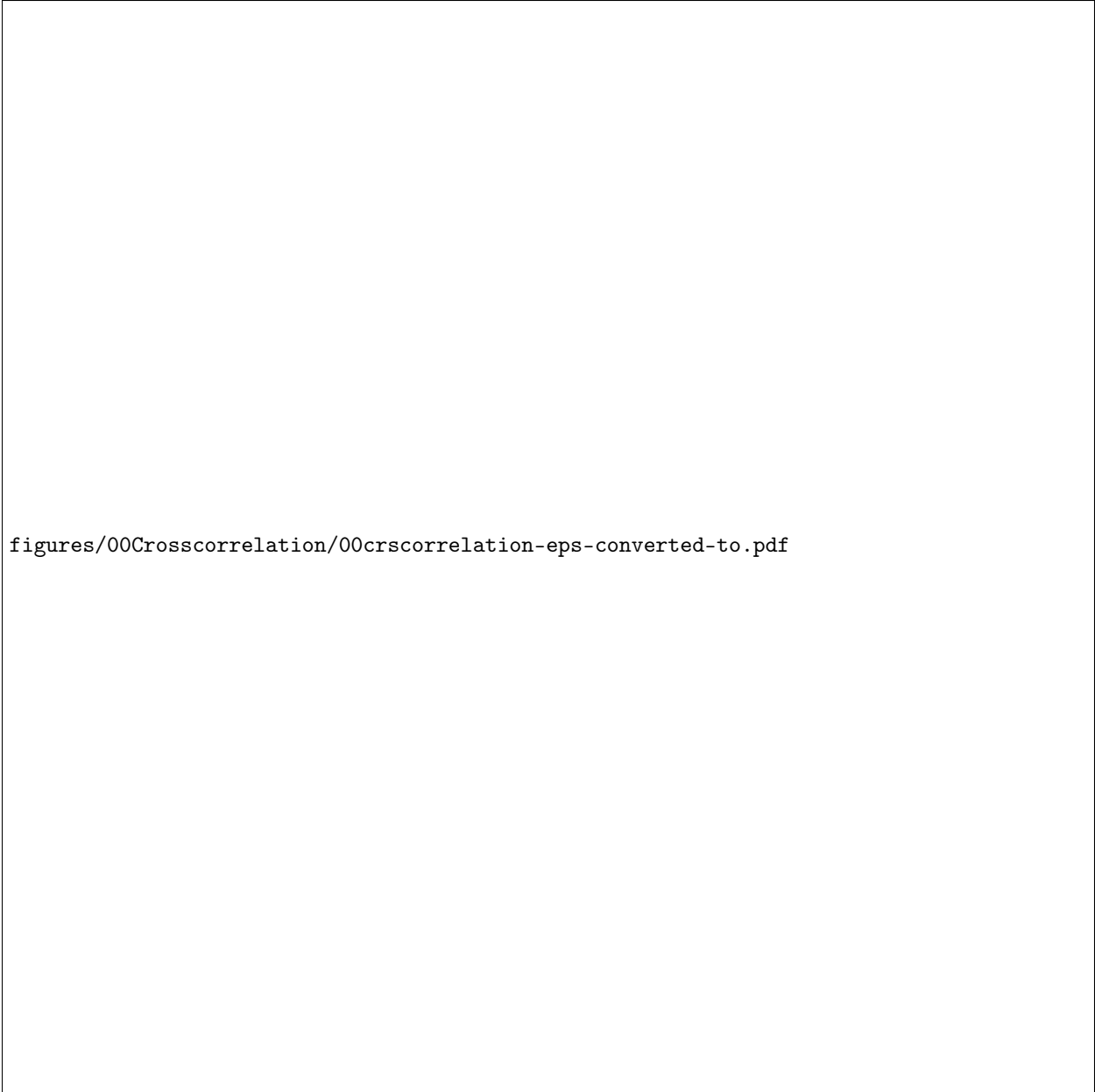

Figure 7: ENSO indices available

Figure 8: Sample cross-correlation functions between the series PDSI and all ENSO indices shown in Figure 7. Numbers indicate the associated lag at the peak value.

The sample cross-correlation function between the series PDSI and all ENSO indices available is shown in Figure 8. Among all ENSO indices, the series ONI resulted with the highest cross-correlation with the PDSI series at a lag of -1 ($\hat{\rho}$=0.43), with the ONI series leading by one time step (one year) the PDSI series. However, since this series is rather short (available from 1950 onwards), we selected the next highly correlated series with PDSI. From all ENSO indices available from 1870 onwards, el Niño3.4 index was selected as having the highest cross-correlation with series PDSI at lag -1 ($\hat{\rho}$=0.35), with the Niño3.4 series leading the PDSI series.

Since the PDO times series is available from year 1900, this was considered the initial year for this analysis. The model training period is the interval (1900-1953) and the model validation period is the interval (1954-2014), which coincides with the validation period used for the ES approach in section .

An ARIMA model was fitted to the PDO series for the training period. An autoregressive model of order 1 (AR(1)) was adequate for the series. Figures 9 a2) presents the sample crosscorrelation function (CCF) between the PDO series (X) and the PDSI series (Y) , and the sample CCF between the pre-whitened X series (residuals after fitting an ARIMA model) and the filtered Y series (after applying the AR(1) filter) presented in Figures 9 a1) .
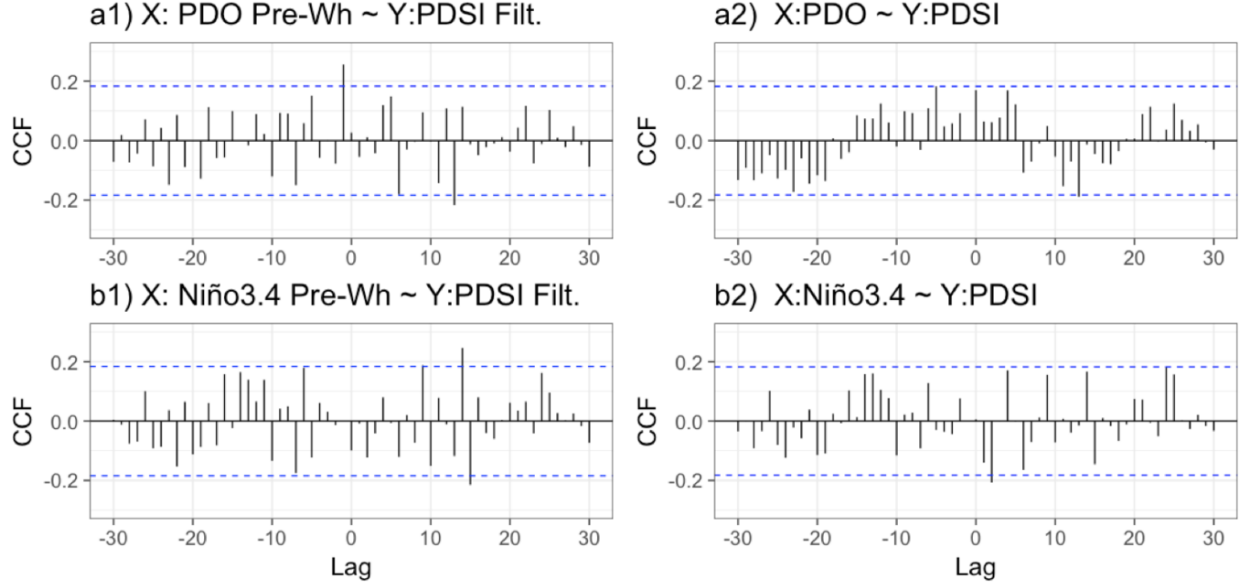

Figure 9: (a1) Sample crosscorrelation function (CCF) between the pre-whitened Pacific Decadal Oscillation (PDO) series denoted as X and the filtered PDSI serie denoted as Y for the training period. (a2) The sample CCF between the PDO series and the PDSI series. (b1) CCF pre-whitened Niño3.4 and the filtered PDSI. (b2) The sample CCF between the Niño3.4 serie and the PDSI serie.

Similarly, an ARIMA model was fitted to the El Niño3.4 series for the training period. An autoregressive model of order 2 (AR(2)) was adequate for the series. Figure 9 b2) presents the sample crosscorrelation function (CCF) between El Niño 3.4 series (X) and the PDSI series (Y), and the sample CCF between the pre-whitened X series (residuals after fitting an ARIMA model) and the filtered Y series (after applying the AR(2) filter) in figure 9 b1).

From the sample CCF functions and according to Box and Jenkins (1970), a transfer function model of order $(r_1, s_1, d_1) = (1, 1, 1)$ for input series $X_1(t) =$ Niño3.4, and order $(r_2, s_2, d_2) = (1, 0, 1)$ for input series $X_2(t) = PDO$, was proposed for this data set. In this case $\alpha_1(B) = (\delta_{01} + \delta_{11}B)B^1/(1 - \omega_{11}B^1)$; and $\alpha_2(B) = (\delta_{02})B^1/(1 - \omega_{12}B^1)$.

The final model to be fitted is of the form:

$$Y_t = \alpha_1 Y_{t-1} + \alpha_2 Y_{t-2} + \alpha_3 Nino3.4_{t-1} + \alpha_4 Nino3.4_{t-2} + \alpha_5 PDO_{t-1} + \eta_t$$

12

Following Shumway and Stoffer (2017a) this model is initially fitted by least squares and the ARIMA model associated to the estimated residuals $\hat{\eta}_t$ is identified. As a second step the model is refitted assuming autocorrelated errors following an ARIMA model with order identified in the previous step. Figure 10 shows the autocorrelation and partial autocorrelation function of the estimated residuals, suggesting a white noise structure with no additional refitting required.
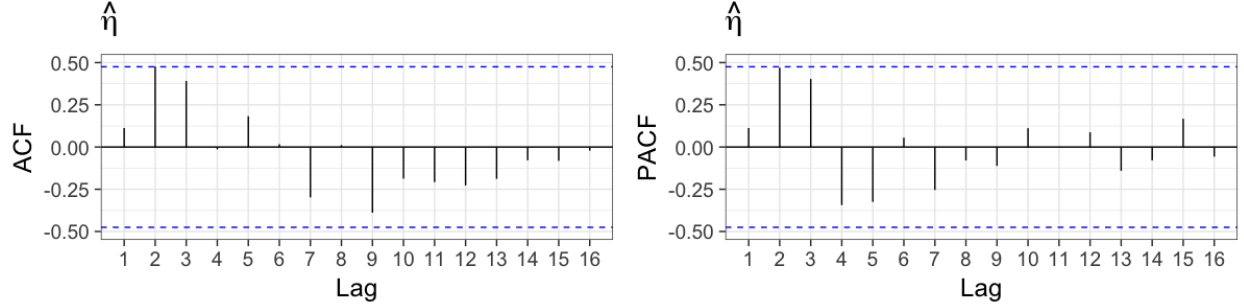

Figure 10: Crosscorrelation and Partial autocorrelation function of the estimated residuals $\hat{\eta}_t$

Figure 11 compares the observed values (black line) with the fitted values for the training period (blue line) and the observed values with the fitted values for the validation period (red line). The 95% prediction intervals are also shown in the analysis.
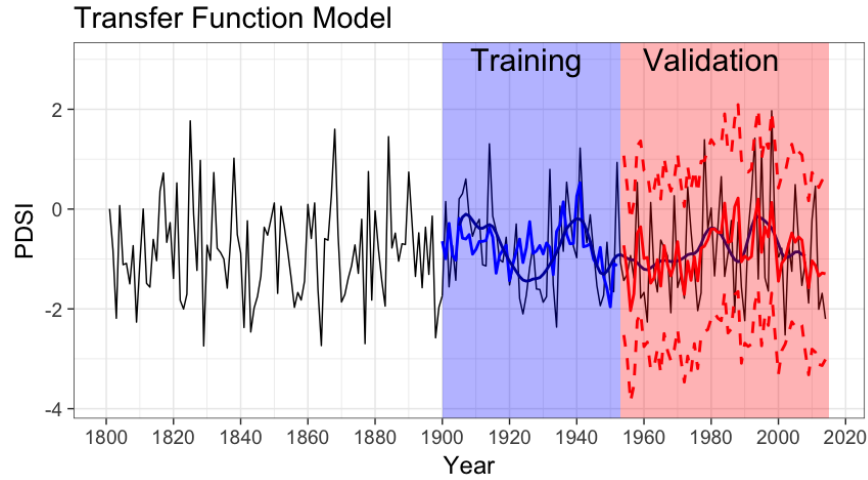

Figure 11: Observed PDSI time series (black line) with the training data set to build the model (blue line) for the period 1900-1953, including the filtered observed values (navy blue). Also comparison between the observed values (black line) and predicted values with the TF model for the validation period (1954-2014)l(red line), including the corresponding 95% confidence intervals (red dash)

The Root Mean Square Error (RMSE) during the validation period is 1.00, while the Mean Absolute Scaled Error (MASE) is 0.95, this means that when comparing with the naive forecast $(Y(t + 1) = Y(t))$ the

predicted values using the transfer function model provide an improvement over the naive forecast. Considering that the training period in this case (1900-1953) is much shorter in comparison with the training period used for the ES method (1800-1953), the transfer function model provides a competitive approach as a forecasting method for the PDSI series.

The histogram and QQ plots of the residuals between the predicted and observed values for the PDSI time series during the validation period show a valid performance of the residuals with an approximate Normal distribution.
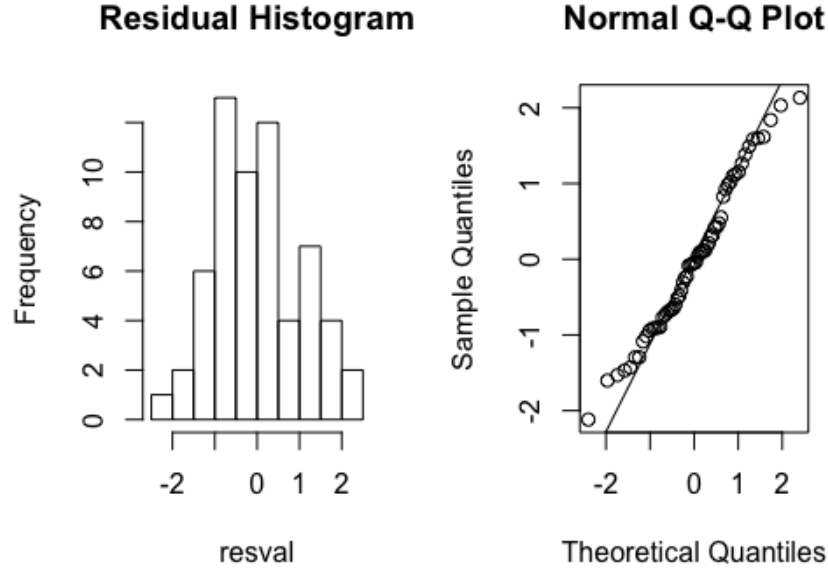

Figure 12: Residual histogram and normal QQ Plot between the PDSI predicted values and observed PDSI time series for the validation period (1954-2014)

Ensemble forecast with the Transfer Function Model

Once the adequacy of the model is assessed, the model is trained over the period 1900-2014 to produce a simulation plume of annual PDSI for the period 2015-2054. El Niño3.4 series and the PDO Series were simulated first, by using the corresponding ARIMA models fitted to the observed time series. Simulations from a model of the form:

$$Y_t = \alpha_1 Y_{t-1} + \alpha_2 Y_{t-2} + \alpha_3 Nino3.4_{t-1} + \alpha_4 Nino3.4_{t-2} + \alpha_5 PDO_{t-1} + \eta_t$$

are presented in Figure 13.

The inter-decadal cycles observed in the ensemble forecast from Figure ?? are not present in this case since a seasonal component has not been considered in the model. The El Niño3.4 series and the PDO series are
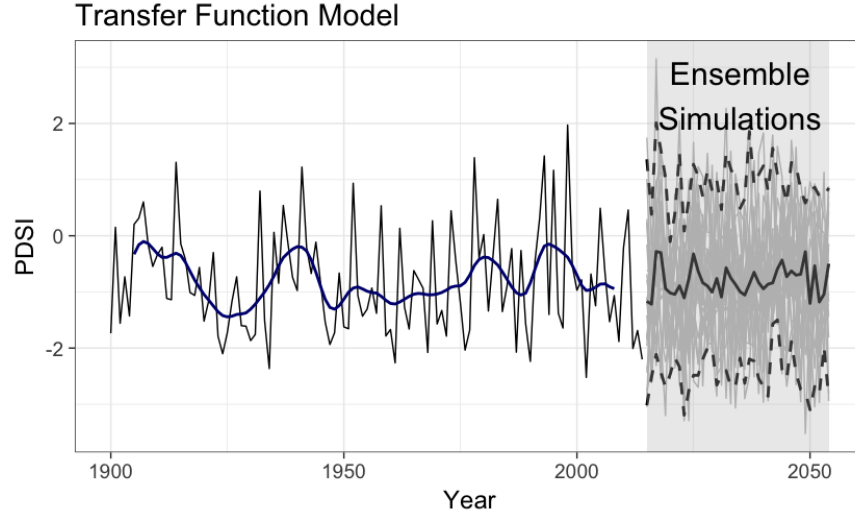
Figure 13: Observed PDSI time series (black line) with the simulation plume (grey lines) for the period 2015-2054, including the filtered observed series (navy-blue line), the median of the simulated values (thick grey line) and the 2.5% (bottom dashed line) and 97.5% quantile (top dashed line) of the simulated values.

assumed independent for simulation which might not be a valid assumption. Figure 14 shows a comparison between the observed PDSI value with the mean ensemble forecast for the ES model and the TF model for the validation period, comparing also the mean future projections for both models. The projection of PDSI over the four future decades (2015-2054) for the ES model lies around the "incipient drought" class, with excursions to "mild drought", while the projections of the TF model remain around the "incipient drought" region.

5. Discussion and concluding remarks

Our results can be useful for water resources planning, and provide and basic knowledge to support further predictive studies beyond the use of Global Climate Models (GCMs, Hazeleger et al. 2015; Ingram 2016), which vary their parameters for climatic simulations under alternative GHG emission scenarios. So far, exponential smoothing approaches were applied almost exclusively in econometric and financial domains (see Hyndman et al., 2008). The major potential cause of bias in exponential smoothing approach is that extrapolative forecasts can differ substantially depending on the time period examined (see Armstrong, 2001a)(**Armstrong, 1999**). However, this bias can be dwindled by identifying long time-series and by comparing forecasts when different starting points are used (ensemble). This is what we have done with an extended series of PDSI data.

Droughts occur over long time spans, and their timing are difficult to identify. This paper takes the challenge to examine a strategy for structuring knowledge about drought dynamics for use in annual PDSI extrapolation for the coming decades.

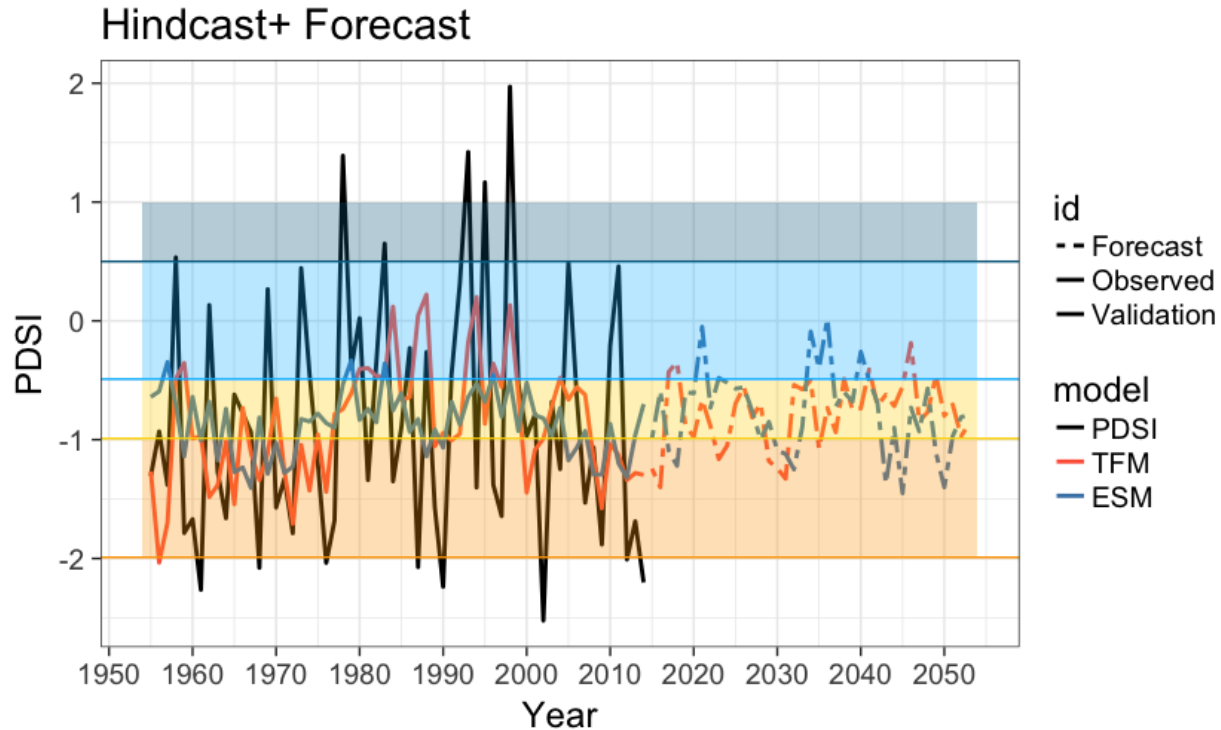| model	RMSE	MASE
Exponential Smoothing	1.00	0.68
Transfer Function	1.00	0.95

Figure 14: Comparison between the Exponential Smoothing model (ESM) forecast and the Transfer Function model (TFM) forecast for the validation period (1954-2014) and the projection period (2015-2055).

Extrapolation suffers when a time series is subject to shocks or discontinuities. Few extrapolation methods account for discontinuities **(Collopy and Armstrong, 1992)**. Instead, when discontinuities occur, extrapolation may lead to large forecast errors. For example, ENSO and Pacifical Decadal Oscillation can lead to experience a strong upward or downward trend of drought **(Colet et al., 2002).** According with **Sheffield and Wood (2008)**, it is plausible that thermal impacts on drought frequency at in the long term are likely to dominate precipitation changes. We could thus expect a monotonic and positive temperature change with increasing drought frequency across a range of drought metrics by the late 21st century. However, the future direction of PDSI series remains uncertain, because uncertain is the direction of its causal forces (temperature and precipitation). This is a challenge in PDSI future extrapolation.

Our empirical forecasts are in agreement with Esfahani and Friedel (2014), whose forecasts suggest the likelihood for the current moderate drought in California to shift to a mid-range condition in 2020 and a constant level of PDSI towards 2060. These authors advocate that California might have reached its equilibrium, the end of a long-memory process, which would be an exception in southwestern U.S., where PDSI would increase.

. . . .

References

Armstrong, J.S., 2001. Combining forecasts. In: Armstrong, J.S. (eds.), Principles of forecasting: a handbook for researchers and practitioners. Kluwer Academic Publishers, Norwell, MA, USA, pp. 1-19.

Arnell N.W., Delaney E.K., 2006. Adapting to climate change: public water supply in England and Wales.

Climatic Change 78, 227-255.

Belov, I., Kabašinskas, A., Sakalauskas, L., 2006. A study models of stock markets. Information Technology and Control 35, 34-56.

Box, G.E.P., Jenkins, G.M., 1976. Time series analysis: forecasting and control. Holden Day, San Francisco, CA, USA, p. 575.

Buishand, T.A. 1982. Some methods for testing the homogeneity of rainfall records. Journal of Hydrology 58, 11-27.

Byun, H.R., Wilhite, D.A., 1999. Objective quantification of drought severity and duration. Journal of Climate 12, 2747-2756.

Chatfield C., 2000. Time-series forecasting. Chapman &C Hall/CRC, Boca Raton London New York Washington, D.C.

Cohen J., Screen J.A., Furtado J.C., Barlow M., Whittleston D., Coumou D., Francis J., Dethloff K., Entekhabi D., Overland J., Jones J., 2014. Recent Arctic amplification and extreme mid-latitude weather. Nature Geoscience 7, 627–637.

Cook, E.R., Seager, R., Cane, M.A., Stahle, D.W., 2007. North American drought: Reconstructions, causes, and consequences. Earth-Science Reviews 81, 93-134.

Dai, A., Trenberth, K.E., Karl, T.R., 1998. Global variations in droughts and west spells: 1900–1995. Geophysical Research Letters 25, 3367-3370.

Dai, A., Trenberth, K.E., Qian, T., 2004. A global dataset of Palmer Drought Severity Index for 1870-2002: relationship with soil moisture and effects of surface warming. Journal of Hydrometeorology 5, 1117-1130.

Diodato, N., 2014. Storminess forecast skills in Naples, Southern Italy. In: Diodato, N., Bellocchi, G. (Eds.), Storminess and environmental change, Springer, Dordrecht, pp. 269-280.

Diodato N., Bellocchi G., 2014. Long-term winter temperatures in central Mediterranean: forecast skill of an ensemble statistical model.Theretical and Applied Climatology 116, 131–146.

Diodato, N., Bellocchi, G., Fiorillo, F., Ventafridda, G., 2017. Case study for investigating groundwater and the future of mountain spring discharges in Southern Italy. Journal of Mountain Science 14, 1791-1800.

(Dotov et al., 2016)

Esfahani, A.A., Friedel, M.J., 2014. Forecasting conditional climate-change using a hybrid approach. Environmental Modelling & Software 52, 83-97.

Fox, D.G. 1981. Judging air quality model performance: a summary of the AMS workshop on dispersion models performance. Bull. Am. Meteorol. Soc., 62, 599-609.

Franses, P.H., 2016. A note on the Mean Absolute Scaled Error. International Journal of Forecasting 32, 20-22.

Fritts, H.C., Lofgren, G.R. and Gordon, G.A. 1979. Variations in climate since 1602 as reconstructed from tree-rings. Quaternary Research 12, 18–46.

Furtado, J.C., Di Lorenzo, E., Schneider, N. and Bond, N.A. 2011. North Pacific decadal variability and climate change in the IPCC AR4 models. Journal of Climate 24: 3049-3067.

Gardner Jr, E.S., 2006. Exponential smoothing: the state of the art - part II. International Journal of Forecasting 22, 637-666.

Jens F., 1988. *Fractals* . New York, Plenum Press, 310 pp.

Hazeleger W., B.J.J.M. van den Hurk, E. Min, G.J. van Oldenborgh, A.C. Petersen, D.A. Stainforth, E. Vasileiadou, L.A. Smith, 2015. Tales of future weather. Nature Climate Change 5, 107–113.

Heshmati G.A., 2007. Vegetation characteristics of four ecological zones of Iran. International Journal of Plant Production 1(2), 215-224.

Holt, C.C., 2004. Forecasting seasonals and trends by exponentially weighted moving averages. International Journal of Forecasting 20, 5-10.

Hyndman, R.J., Koehler, A.B., 2006. Another look at measures of forecast accuracy. Int. J. Forecast. 22, 679-688.

Hyndman, R.J., Koehler, A.B., Ord, J.K., Snyder, R.D., 2008. Forecasting with exponential smoothing: the state space approach. Berlin, Springer, p. 362.

Ingram W., 2016. Extreme precipitation: Increases all round. Nature Climate Change 6, 443–444.

Kaklauskas, L., Sakalauskas, L., 2013. Study of on-line measurement of traffic self-similarity. Central European Journal of Operations Research 21, 63-84.

Kamruzzaman M., Beecham S., Metcalfe A.V., 2010. Non-stationarity in rainfall and temperature in the Murray Darling Basin. Hydrol. Process. 25, 1659–1675.

Karagiannis, T., Faloutsos, M., Riedi, R., 2002. Long-Range dependence: Now you see it now you don't! In: Proceedings of the Global Telecommunications Conferenc 'GLOBECOM '02", IEEE, Vol. 3, Taipei, Taiwan. http://www.stat.rice.edu/~riedi/Publ/PDF/LRDsee.pdf

Karl, T.R., Koscielny, A.J., 1982. Drought in the United States. Journal of Climatology 2, 313-329.

Knudsen, M.F., Seidenkrantz, M.-S., Jacobsen, B.H., Kuijpers, A., 2011. Tracking the Atlantic Multidecadal Oscillation through the last 8,000 years. Nature Communications 2, 178, doi: 10.1038/ncomms1186.

Knutti, R., Krähenmann, S, Frame, D.J., Allen, M.R., 2008. Comment on "Heat capacity, time constant, and sensitivity of Earth's climate system" by S. E. Schwartz. Journal of Geophysical Research 113, D15103, doi:10.1029/2007JD009473.

Koster, R.D., Dirmeyer, P.A., Guo, Z., Bonan, G., Chan, E., Cox, P., Gordon, C.T., Kanae, S., Kowalczyk, E., Lawrence, D. et al., 2004. Regions of strong coupling between soil moisture and precipitation. Science 305, 1138-1140.

Leith, C.E. 1975. Climate response and fluctuation-dissipation. Journal of the Atmospheric Sciences 32, 2022-2026.

Lin, L., Wang, Z., Xu, Y., Fu, Q., 2016. Sensitivity of precipitation extremes to radiative forcing of greenhouse gases and aerosols. Geophysical Research Letters 43, 9860-9868.

McClain, J.O., 1974. Dynamics of exponential smoothing with trend and seasonal terms. Management Science 20, 1300-1304.

Montgomery D.C., Jennings C.L., Kulachi M., 2008. Introduction to time-series analysis and forecasting. Wiley, 445 pp.

Mulligan M., Wainwright J., 2004. Modelling and Model Building. In: Environmental Modelling, Wainwright J. and Mulligan M. (eds.), Wiley, pp. 7-73.

Newbold P., Granger C.W.J., 1974. Experience with forecasting univariate time series and the combination of forecasts. J.R. Staist. Soc. A, 137, 131-146.

Palmer, WC, 1965. Meteorological drought. Research Paper No. 45. Office of Climatology. U.S. Weather Bureau: Washington, DC, USA.

Perry CA, Hsu KJ (2000) Geophysical, archaeological, and historical evidence support a solar-output model for climate change. P Natl Acad Sci USA 97, 1244-12438.

Quassim M.S., Attia A.F., 2005. Forecasting the global temperature trend according to the predicted solar activity during the next decades. Memoire della Società Astronomica Italiana 76:1030-1033.

Quian B, Rasheed K (2004) Hurst exponent and financial market predictability. 2nd IASTED International Conference on Financial Engineering and Applications, 8-11 November, Cambridge, MA.

Roe G.H., Baker, M.B., 2007. Why is climate sensitivity so unpredictable? Science, 318, 629-631.

Scafetta N., 2010. Empirical evidence for a celestial origin of the climate oscillations and its implications. Journal of Atmospheric and Solar Terrestrial Physics 72, 951-970.

Shabbar, A., Skinner, W., 2004. Summer drought patterns in Canada and the relationship to global sea surface temperatures Journal of Climate 17, 2866-2880.

Smith T.S., Karl T.R., Reynolds R.W. (2002) How accurate are climate simulations? Science 296, 483-484.

Sheng H, Chen YQ (2009) Robustness analysis of the estimators for noisy long-range dependent time series. ASME 2009 International Design Engineering Technical Conferences & Computers and Information in Engineering Conference, San Diego, CA.

Shumway and Stoffer (2017b)

Stern P.C, Easterling W.E., 1999. Making Climate Forecasts Matter. National Academy of Sciences, 192 pp.

Stroe-Kunold E., Stadnytska T., Werner J., Braun S., 2009 Estimating long-range dependence in time series: an evaluation of estimators implemented in R. Behavior Research Methods 41, 909-923.

Tatli, H., 2015. Detecting persistence of meteorological drought via the Hurst exponent. Meteorological Applications 22, 763-769.

(Taylor, 2003)

Trenberth, K. E., and J. T. Fasullo, 2010. Tracking Earth's energy. Science 328, 316-317.

van der Schrier, G.,. Briffa, K.R., Osborn, T.J., Cook, E.R., 2006. Summer moisture availability across North America. Journal of Geophysical Research 111, D11102.

Van Oldenborgh, G. J., S. S. Drijfhout, A. van Ulden, R. Haarsma, A. Sterl, C. Severijns, W. Hazeleger, and H. Dijkstra, 2009. Western Europe is warming much faster than expected. Clim. Past, 5, 1-12, doi:10.5194/cp-5-1-2009.

Wells, N., Goddard, S., Hayes, M.J., 2004. A self-calibrating Palmer Drought Severity Index. Journal of Climate 17, 2335-2351.

Weaver AJ, Hillaire-Marcel C, 2004. Global warming and the next ice age. Science 304, 400-402.

Wessa P., 2012. Free Statistics Software, Office for Research Development and Education, version 1.1.23-r7, URL http://www.wessa.net.

Woodhouse, C.A., Kunkel, K.E., Easterling, D.R., Cook, E.R., 2005. The twentieth-century pluvial in the western United States. Geophysical Research Letters 32, L07701.

Yin, X.-A., Yang, X.-H., Yang, F.-Z., 2009. Using the R/S method to determine the periodicity of time series. Chaos, Solitons & Fractals 39, 731-745.

Wichard, J.D., Merkwirth, C., 2005. Robust long term forecasting of seasonal time series. http://www.j-wichard.de/publications/iwann2005.pdf

Zhang X., Francis W. Zwiers, Guilong Li, Hui Wan, Alex J. Cannon, 2017. Complexity in estimating past and future extreme short-duration rainfall. Nature Geoscience 10, 255–259.

References

T. M. Addiscott and A. P. Whitmore. *Computer simulation of changes in soil mineral nitrogen and crop nitrogen during autumn winter and spring.* The Journal of Agricultural Science, 109(01):141, aug 1987. doi: 10.1017/s0021859600081089. URL https://doi.org/10.1017%2Fs0021859600081089.

J. Scott Armstrong. *Combining Forecasts.* In International Series in Operations Research & Management Science, pages 417–439. Springer US, 2001a. doi: 10.1007/978-0-306-47630-3_19. URL https://doi.org/10.1007%2F978-0-306-47630-3_19.

J. Scott Armstrong. *Combining Forecasts.* In International Series in Operations Research & Management Science, pages 417–439. Springer US, 2001b. doi: 10.1007/978-0-306-47630-3_19. URL https://doi.org/10.1007%2F978-0-306-47630-3_19.

Kabašinskas A. Sakalauskas L. Belov, I. *A study models of stock markets.* Information Technology and Control, 35, 2006.

G. E. P. Box and G. M. Jenkins. *Time series analysis: Forecasting and control.* San Francisco: Holden-Day., 1970.

G. E. P. Box and G. M. Jenkins. *Time series analysis: forecasting and control.* Holden Day, San Francisco, CA, USA, 575, 1976.

T.A. Buishand. *Some methods for testing the homogeneity of rainfall records.* Journal of Hydrology, 58 (1-2):11–27, aug 1982. doi: 10.1016/0022-1694(82)90066-x. URL https://doi.org/10.1016%2F0022-1694%2882%2990066-x.

Hi-Ryong Byun and Donald A. Wilhite. *Objective Quantification of Drought Severity and Duration.* Journal of Climate, 12(9):2747–2756, sep 1999. doi: 10.1175/1520-0442(1999)012<2747:oqodsa>2.0.co;2. URL https://doi.org/10.1175%2F1520-0442%281999%29012%3C2747%3Aoqodsa%3E2.0.co%3B2.

Chris Chatfield. *Time-Series Forecasting.* Chapman and Hall/CRC, oct 2000. doi: 10.1201/9781420036206. URL https://doi.org/10.1201%2F9781420036206.

E. R. Cook, R. Seager, M. A. Cane, and D. W. Stahle. *North American drought: Reconstructions, causes, and consequences.* Earth-Science Reviews, 81:93–134, 2007.

A. Dai, K. E. Trenberth, and T. R. Karl. *Global variations in droughts and west spells: 1900–1995.* Geophysical Research Letters, 25:3367–3370, 1998.

A. Dai, K. E. Trenberth, and T. Qian. *A global dataset of Palmer Drought Severity Index for 1870-2002: relationship with soil moisture and effects of surface warming.* Journal of Hydrometeorology, 5:1117–1130, 2004.

Lelys B. de Guenni, Mariangel Garcia, Angel G. Munoz, Jose L. Santos, Alexandra Cedeo, Carlos Perugachi, and Jose Castillo. *Predicting monthly precipitation along coastal Ecuador: ENSO and transfer function models.* Theoretical and Applied Climatology, 129(3-4):1059–1073, may 2016. doi: 10.1007/s00704-016-1828-4. URL https://doi.org/10.1007%2Fs00704-016-1828-4.

N. Diodato. *Storminess forecast skills in Naples, Southern Italy.* In Bellocchi and N., editor, Diodato, N., Bellocchi, G. (Eds.), pages 269–280. Storminess and environmental change, Springer, Dordrecht, 2014.

N. Diodato and G. Bellocchi. *Long-term winter temperatures in central Mediterranean: forecast skill of an ensemble statistical model.* Theretical and Applied Climatology, 116:131–146, 2014.

N. Diodato, G. Bellocchi, F. Fiorillo, and G. Ventafridda. *Case study for investigating groundwater and the future of mountain spring discharges in Southern Italy.* Journal of Mountain Science, 14:1791–1800, 2017.

D. G. Dotov, B. G. Bardy, and Dalla Bella. *The role of environmental constraints in walking: Effects of steering and sharp turns on gait dynamics.* Scientific Reports, 6:28374, 2016.

A. A. Esfahani and M. J. Friedel. *Forecasting conditional climate-change using a hybrid approach.* Environmental Modelling & Software, 52:83–97, 2014.

D. G. Fox. *Judging air quality model performance: a summary of the AMS workshop on dispersion models performance.* Bull. Am. Meteorol. Soc., 62:599–609, 1981.

P. H. Franses. *A note on the Mean Absolute Scaled Error.* International Journal of Forecasting, 32:20–22, 2016.

Daniel Griffin and Kevin J. Anchukaitis. *How unusual is the 2012-2014 California drought?* Geophysical Research Letters, 41(24):9017–9023, dec 2014a. doi: 10.1002/2014gl062433. URL https://doi.org/10.1002%2F2014gl062433.

Daniel Griffin and Kevin J. Anchukaitis. *How unusual is the 2012-2014 California drought?* Geophysical Research Letters, 41(24):9017–9023, dec 2014b. doi: 10.1002/2014gl062433. URL https://doi.org/10.1002%2F2014gl062433.

W. Hazeleger, B. J. J. M. van den Hurk, E. Min, G. J. van Oldenborgh, A. C. Petersen, D. A. Stainforth, E. Vasileiadou, and L. A. Smith. *Tales of future weather.* Nature Climate Change, 5:107–113, 2015.

C. C. Holt. *Forecasting seasonals and trends by exponentially weighted moving averages.* International Journal of Forecasting, 20:5–10, 2004.

R. J. Hyndman, A. B. Koehler, J. K. Ord, and R. D. Snyder. *Forecasting with exponential smoothing: the state space approach.* Berlin, Springer, p. 362, 2008.

Rob J. Hyndman and Anne B. Koehler. *Another look at measures of forecast accuracy.* International journal of forecasting, 22(4):679–688, 2006.

William Ingram. *Extreme precipitation: Increases all round.* Nature Climate Change, 6:5, 2016.

L. Kaklauskas and L. Sakalauskas. *Study of on-line measurement of traffic self-similarity.* Central European Journal of Operations Research, 21:63–84, 2013.

Thomas Karagiannis, Michalis Faloutsos, and Rudolf H. Riedi. *Long-range dependence: now you see it, now you don't!* In Global Telecommunications Conference. 2002. GLOBECOM'02. IEEE. Vol. 3. IEEE, 2002.

T. R. Karl and A. J. Koscielny. *Drought in the United States.* Journal of Climatology, 2:313–329, 1982.

R. D. Koster, P. A. Dirmeyer, Z. Guo, G. Bonan, E. Chan, P. Cox, C. T. Gordon, S. Kanae, E. Kowalczyk, and D. al. Lawrence. *Regions of strong coupling between soil moisture and precipitation.* Science, 305:1138–1140, 2004.

J. O. McClain. *Dynamics of exponential smoothing with trend and seasonal terms.* Management Science, 20:1300–1304, 1974.

D.C. Montgomery, C.L. Jennings, and M. Kulachi. *Introduction to Time - Series Analysis and Forecasting.* Wiley, 2008.

W. C. Palmer. *Meteorological drought. Research Paper No. 45, Office of Climatology US.* Weather Bureau, Washington, DC, 1965.

B. Quian and K. Rasheed. *Hurst exponent and financial market predictability.* In 2nd IASTED International Conference on Financial Engineering and Applications, 2004.

Amir Shabbar and Walter Skinner. *Summer Drought Patterns in Canada and the Relationship toGlobal Sea Surface Temperatures.* Journal of Climate, 17(14):2866–2880, 2004.

H. Sheng and Y. Q. Chen. *Robustness analysis of the estimators for noisy long-range dependent time series.* ASME, 2009, 2009.

Robert H. Shumway and David S. Stoffer. *Time Series Analysis and Its Applications.* Springer International Publishing, 2017a. doi: 10.1007/978-3-319-52452-8. URL https://doi.org/10.1007%2F978-3-319-52452-8.

Robert H. Shumway and David S. Stoffer. *Time Series Analysis and Its Applications.* Springer International Publishing, 2017b. doi: 10.1007/978-3-319-52452-8. URL https://doi.org/10.1007%2F978-3-319-52452-8.

H. Tatli. *Detecting persistence of meteorological drought via the Hurst exponent.* Meteorological Applications, 22:763–769, 2015.

J. W. Taylor. *Exponential smoothing with a damped multiplicative trend.* International Journal of Forecasting, 19:715–725, 2003.

N. Wells, S. Goddard, and M. J. Hayes. *A self-calibrating Palmer Drought Severity Index.* Journal of Climate, 17:2335–2351, 2004.

P. Wessa. *Free Statistics Software.* Office for Research Development and Education, version, 2012. URL http://www.wessa.net. version 1.1.23-r7.

Jörg Wichard and Christian Merkwirth. *Robust Long Term Forecasting of Seasonal Time Series.* 2005. URL http://www.j-wichard.de/publications/iwann2005.pdf.

Connie A. Woodhouse et al. *The twentieth-century pluvial in the western United States.* Geophysical Research Letters, 32:7, 2005.

X.-a. Yin, X.-h. Yang, and F.-z. Yang. *Using the R/S method to determine the periodicity of time series.* Chaos, Solitons & Fractals, 39:731–745, 2009.